Structural Engineering and Mechanics, Vol. 41, No. 4 (2012) 441-458 441
DOI: http://dx.doi.org/10.12989/sem.2012.41.4.441

Nonlinear shear strength of pre-stressed concrete beams

Alireza Rahai* and A. Shokoohfar

Department of Civil Engineering, Amir Kabir University of Technology, Tehran 1591634311, Iran

(Received February 9, 2010, Revised August 8, 2011, Accepted January 20, 2012)

Abstract. The shear strength is an important factor in the design of prestressed concrete beams. Therefore, researchers have utilized various methods to determine the shear strength of these elements for the design purposes. To evaluate some of the proposed theoretical methods, numerous models of post-tensioned beams with or without vertical prestressing are selected and analyzed using the finite element method and assuming nonlinear behavior for the materials. In this regard the validity of modeling is evaluated based on some tests results. In the second part of the study two beam specimens are built and tested and their load-deformation curve and cracking pattern are studied. The analytical results consist of compressive strut slope and mid span load deflection are compared with some experimental results, and the results of some codes' formulas. Finally comparing the results of nonlinear analysis with the experimental values, a new formula is proposed for determining strut slopes in prestressed concrete beams.

Keywords: shear strength; prestressed concrete; vertical prestressing; strut slope; crack pattern; testing; truss models

1. Introduction

In prestressed concrete beams, the exertion of a prestress compressive force causes a reduction in diagonal tensile stresses and changes the direction of the slope of the diagonal compressive stresses. Using inclined or curved tendons, the vertical component of prestressing force, which is in opposite direction of external loads, reduces the effective shear on the section. These factors increase the shear capacity of prestressed concrete beams whereas in reinforced concrete beams no such increase exists. In some cases, vertical prestressing is also used to create compressive stress in the web.

In order to investigate the shear strength of concrete beams, different theories have been put forth. Ritter (1899) was the first researcher who proposed a simple truss model for shear analysis. His model was very conservative, neglecting the concrete contribution in shear strength and assuming the diagonal compression strut slope to be equal to 45 degrees. Using experimental results, (Withey 1907, Talbot 1909) pointed to the over-estimating results of Ritter's model. Despite these observations, Morsch (1920) used Ritter's model to study the shear and torsional strength of concrete beams.

*Corresponding author, Professor, E-mail: rahai@aut.ac.ir

The angle of inclination of the diagonal compressive stress is often less than 45 degrees, and the assumption of 45 degrees for this angle is very conservative. Discussing this problem, Morsch (1922) stated, “It is absolutely impossible to determine mathematically the slope of the secondary inclined cracks according to which one can design the stirrups.” Just seven years after this statement, another German engineer, Wagner (1929), solved a similar problem while dealing with the shear design of “stressed skin” aircraft. To determine the inclination angle of the diagonal tension, Wagner considered the deformation of the system. He assumed this angle in the buckled thin metal skin which coincides with the angle of inclination of the principal tensile strain as determined from the deformations of the skin, the transverse frames, and the longitudinal stringers. This approach came to be referred to as the tension field theory.

The shear design procedures which determine the angle of θ by considering the deformations of the transverse reinforcement, the longitudinal reinforcement, and the diagonally strut are presented as compression field approaches.

Other methods for determining the θ angle applicable to all loading cases and based on Wagner’s procedure were developed by Collins (1980). This procedure was called the compression field theory (CFT). Based on the results from a series of intensively instrumented beams, they suggested a relationship between the principal compressive stress and the principal compressive strain for diagonally cracked concrete. Using these assumptions, equilibrium conditions, and compatibility relationships, they could determine the angle of θ. The CFT theory assumes that after cracking there will be no tensile stress in the concrete. Tests on reinforced concrete elements have carried out by Vechio and Collins (1986) demonstrated that even after extensive cracking, tensile stresses exists in the cracked concrete to resist shear stresses. It was found that after cracking, the average principal tensile stress in the concrete decreases as the principal tensile strain increases.

Vechio and Collins (1986) have introduced the modified compression field theory (MCFT) which considers the effect of the tensile stresses in the cracked concrete. The equilibrium conditions, the compatibility relationships, the stress-strain relationships of reinforcement and cracked concrete enable one to determine the average stresses, the average strains, and the angle θ. Bentz *et al.* (2006) have suggested Simplified MCFT that presents a new simplified analytical method that can predict the shear strength of RC members in a method suitable for “back of the envelope” calculations.

Ramirez (1991) also initiated the modified truss- model approach for beams by similar assumptions. More simple and accurate truss-tie methods such as modified strut-and-tie model (MSTM) for simply supported prestressed concrete deep beams are proposed by Wang (2008).

In addition to above mentioned method there are some new strut-tie models such as Bottle shaped struts method suggested by Brown and Oguzhan (2006) which presents equilibrium based approach to determining the necessary amount of transverse reinforcement.

In this paper the compressive strut angle has been evaluated based on stress field method. The stress field method which is developed by Muttoni *et al.* (1997) is an equilibrium solution based on the lower bound theorem of plasticity, which is suitable for the dimensioning of reinforced and prestressed concrete members.

The shear strength of reinforced and prestressed concrete beams has been studied in three different stages: reinforced concrete, prestressed concrete, and prestressed concrete with vertical prestressing using a numerical study based on continuous stress field theory introduced by Ruiz and Muttoni (2008).

Diverse methods can be used for concrete damage simulation such as constitutive model suggested by Rabczuk and Eibl (2005) which is a fictitious smeared crack model in tension and a non local scalar damage model in compression, But in this research concrete damage plasticity presented by Lee and Fenves (1998), which is the most suitable model for nonlinear analysis, is used.

Several tests have been performed in AUT labs to determine strut inclination and bending strength. The test results are used to validate the nonlinear analysis accuracy.

2. Research significance

Strut and tie models have seen increased use in recent years. This paper focuses on a more realistic determination of the angle of orientation of the compression struts in prestressed concrete beams. The findings should be of interest to researchers as well as practicing engineers involved in analysis and design of prestressed concrete beams.

3. Numerical analysis validation using muttoni and fernandez test results

Ruiz and Muttoni (2007) have done six tests on beams extracted from Viadotto Sopra Viaduct le

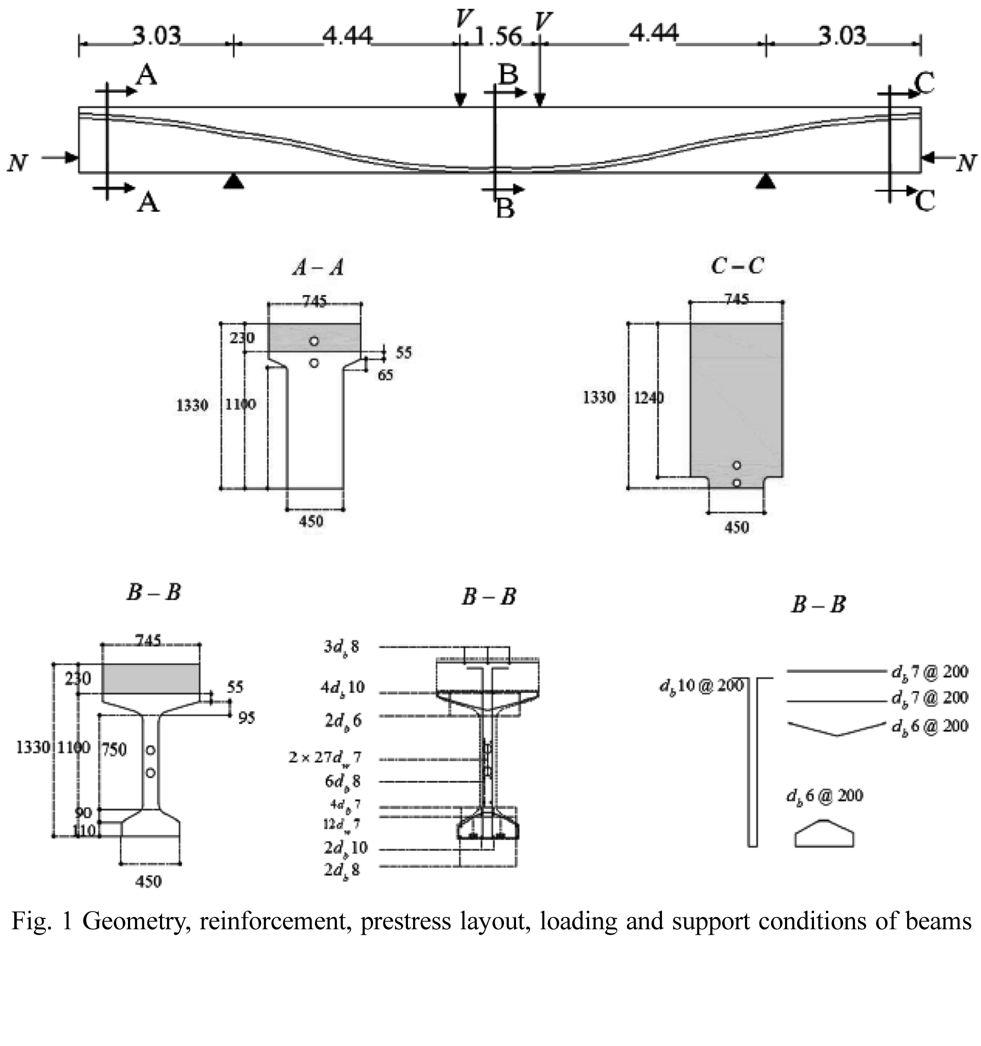

Fig. 1 Geometry, reinforcement, prestress layout, loading and support conditions of beams

Cantine in Switzerland in order to study their behavior and to investigate the effect of vertical prestressing on web cracking. In this research the validation is performed using one of the beams test results. The main geometric properties of the test beam are shown in Fig. 1. The concrete compressive strength in the slab and precast element are f_{cm} = 48.2 and 53.4 MPa respectively, and the elastic modulus is E_{cm} = 33500 MPa. Mechanical properties of steel elements are presented in Table 1. According to Measurements were taken by Czaderski and Motavalli (2006) for the various specimens have been shown that a mean value of σ_{pe} is 530 MPa this means that only 45% of the initial prestress was remained.

The results contain, load-deflection curve at mid span, horizontal strain σ_x along upper flange, compressive strut angle along the beam, and failure mode of specimen. The results of numerical and experimental study are shown in Figs. 2 to 6.

According to Fig. 2, test data have been recorded just at loading stage but the numerical analysis results is related to both prestressing and loading stages, in this reason the zero values for deflection aren't the same. The difference between numerical and experimental results depends on concrete behavioral model which is based on stress-strain diagrams obtained from some compressive and tensile test results.

Table 1 Measured reinforcing and prestressing steel properties

Type	d_b, d_w, mm	f_{ym}, 0.2%, MPa	f_{tm}, MPa	$\varepsilon_{u,\%}$	NO.
			Web and lower flange		
Cold worked	8	624	747	5.7	5
Cold worked	10	582	730	4.9	5
			Deck slab		
Hot rolled	12	392	544	15.2	3
Hot rolled	20	374	521	11.5	1
Hot rolled	26	371	560	15.5	1
			Prestressing Wires of post tensioning tendons		
Wires	7	1457	1738	4.5	3

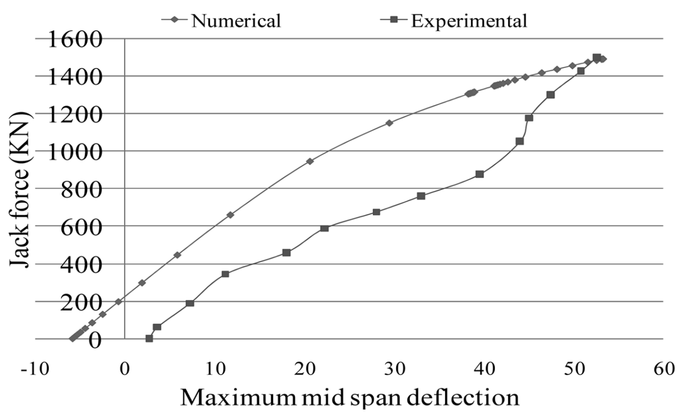

Fig. 2 Load deflection of mid span from numerical and experimental results

Compressive longitudinal strains were measured to be larger than 2% in the upper flange. It can be noted that plane sections remain approximately plane except in the vicinity of tendons where a significant increase in the longitudinal strains is observed.

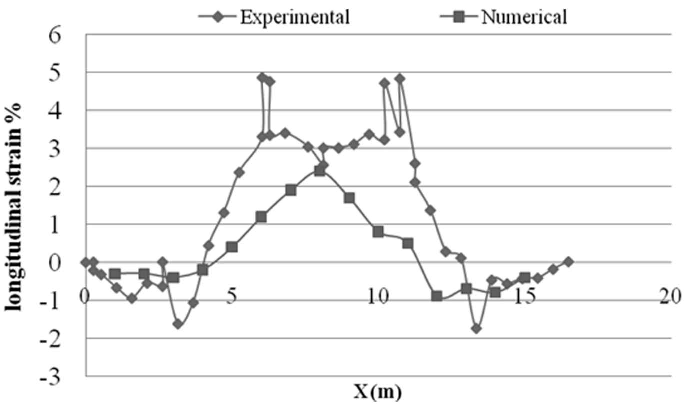

Fig. 3 Longitudinal strain in upper flange

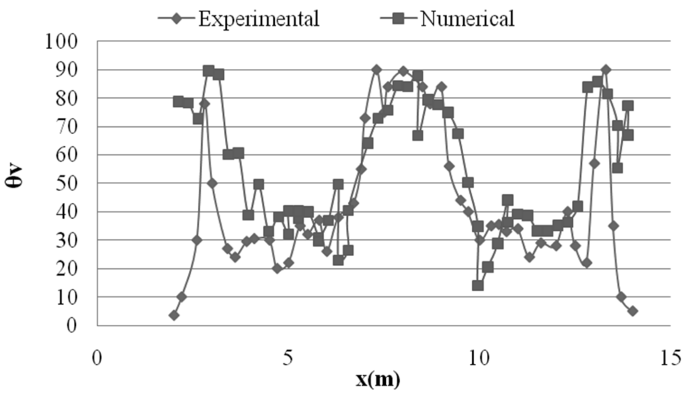

Fig. 4 Compressive strut angle

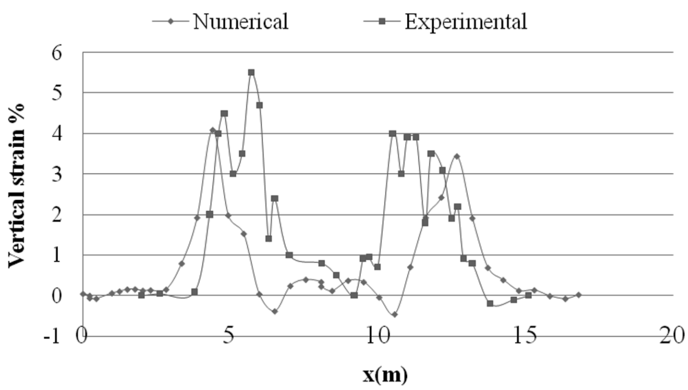

Fig. 5 Vertical strain along line at two-thirds of beam height

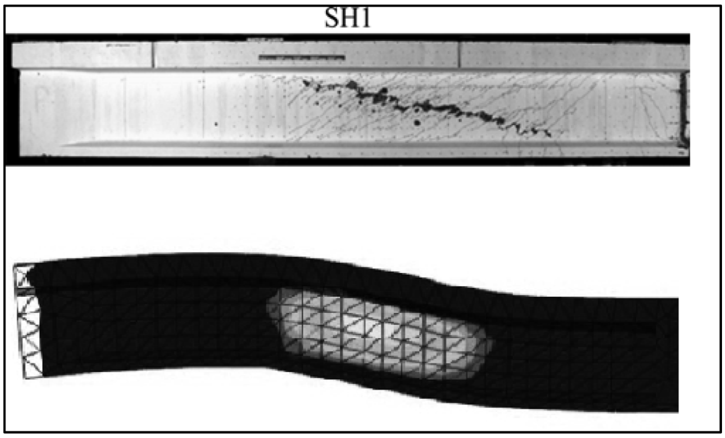

Fig. 6 Failure mode in experiment and analysis

Table 2 A summary of verification results

Name	Maximum mid span deflection (mm)	Maximum bearing capacity (KN)	Failure mode
Numerical model	53.12 mm	V = 1491 KN, N = 3580 KN	Web concrete spalling
Experimental model	52.6 mm	V = 1491 KN, N = 3580 KN	Web concrete spalling

In the beams web, vertical strains larger than 5% were measured, indicating extensive stirrup yielding. Also, a vertical strain is not uniform in every section, with larger strains above the tendon region. These results indicate that the strain localization develops at the level of the tendons which are actively interacting in the structural response of the member. Because of tendon prestressing substitution with equivalent loads, the strain localization effect wasn't observed in numerical results. The compressive strut angle variation along the beam is shown in Fig. 4. A summary of mentioned results is presented in Table 2.

4. Experimental campaign

Two tests were performed using beam specimens built in structural laboratory of AUT. The beam section geometry was 400×200 mm thick, with one post-tensioning tendon placed in 20 mm diameter plastic conduit. The post-tensioning parabolic tendon consists of 7 wires of Φ2 mm was tensioned at ninety days after pouring of concrete.

The tests aimed at investigating the actual behavior of these members under two point loading conditions and numerical study verification (Fig. 7). The total beam length, the distance between supports, and the distance between loading points were 4.4 m, 3 m, 1.8 m respectively. The concrete mechanical strengths were evaluated by preparing several cylinder and prism samples. A summary of the results obtained is presented in Table 3. The concrete elastic modulus was 31622 MPa.

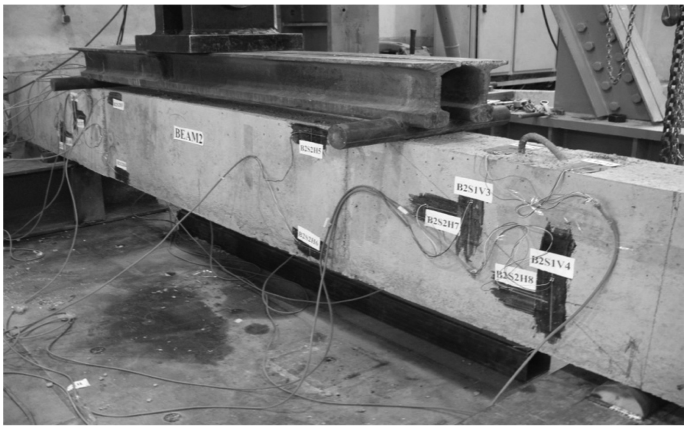

Fig. 7 AUT University tests

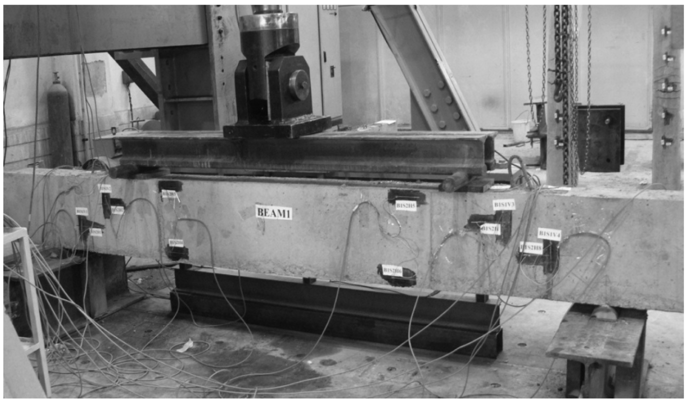

Fig. 8 Strain gauge layout

Table 3 Mechanical properties of concrete specimens

Type and Number of specimens	7 days compressive test results (Mpa)	28 days compressive test results (Mpa)	120 days compressive test results (Mpa)
Cubic-3	33	44	48
Cylindrical-3	27	36	40

In beams construction four 12 mm longitudinal bars with f_{yk} = 400 MPa, and 8 mm stirrups distanced at 300 mm were used. Also tendons cross sectional area, minimum rupture load, and yield tensile stress were 94 mm^2, 116 KN and 1240 MPa respectively. In order to minimize the draw in effects and prestressing relaxation, the tendons were tensioned in three stages. The ultimate equivalent amount of prestressing was 100 KN and detailed information about tendon tensioning is presented in Table 4.

The test setup is shown in Fig. 8. The strains in the three sides of the test beam were measured

Table 4 Cable prestressing stages

Cable type	Effective prestressing force (KN)	First stage tensioning stress (Mpa)	Cable elongation at first stage (mm)	Second stage tensioning stress (Mpa)	Cable elongation at second stage (mm)	Third stage tensioning stress (Mpa)	Cable elongation at third stage (mm)
T13	100	5	1	15	5	21.2	13

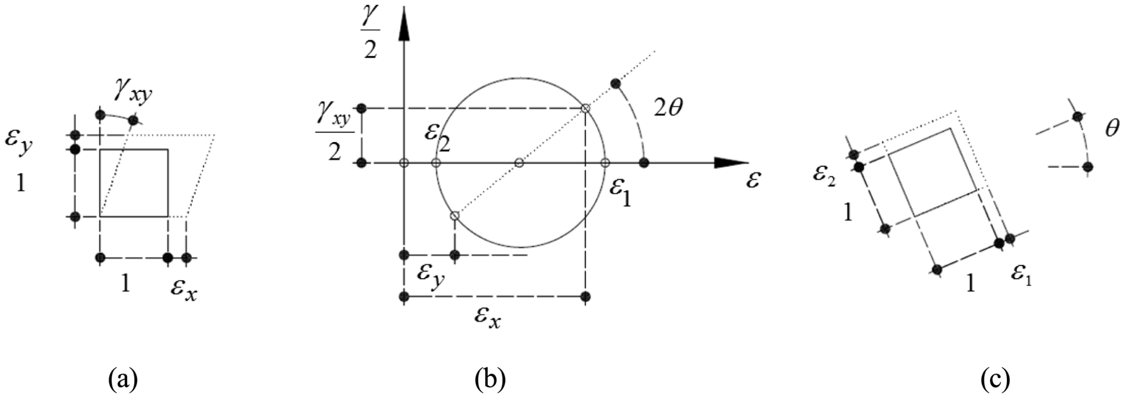

Fig. 9 Strut inclination determination by means of Mohr's circle (a) strains; (b) Mohr's circle and principal strains; (c) directions of principal strains

with PL-60-11 strain gauges. Based on these results, the principal compressive strain direction could be determined. Since this type of strain gauge only measures strains in one direction, the compressive strut angles are obtained by means of Mohr's circle as shown in Fig. 9 with the strain amounts in three directions using the below formula

$$\tan 2\theta = \frac{\gamma_{xy}}{\varepsilon_x - \varepsilon_y} \tag{1}$$

5. Failure mode

The test specimens were tested as shown in Fig. 7. Initial cracks have been occurred in the distance between support and loading points where the shear and bending moment are maximum and minimum respectively. Both specimens were failed by tensile shear failure and spalling of concrete in the loading point zone. The failure mode of the test beams, which are similar to the results of numerical analysis and approve them, is shown in Fig. 10.

The load-mid span deflection curves are presented in Fig. 11. At failure, significant strains were measured in both sides of the beam. Compressive strut angles are presented in Table 5. The nonlinear analysis results are also compared with test results in Fig. 11 and Table 5.

Ultimate load and maximum mid span deflection of TEST1, TEST2 and nonlinear analysis are 310 KN, 360 KN, 333 KN and 40.82 mm, 43.2 mm, 44.7 mm respectively, which have an acceptable similarity.

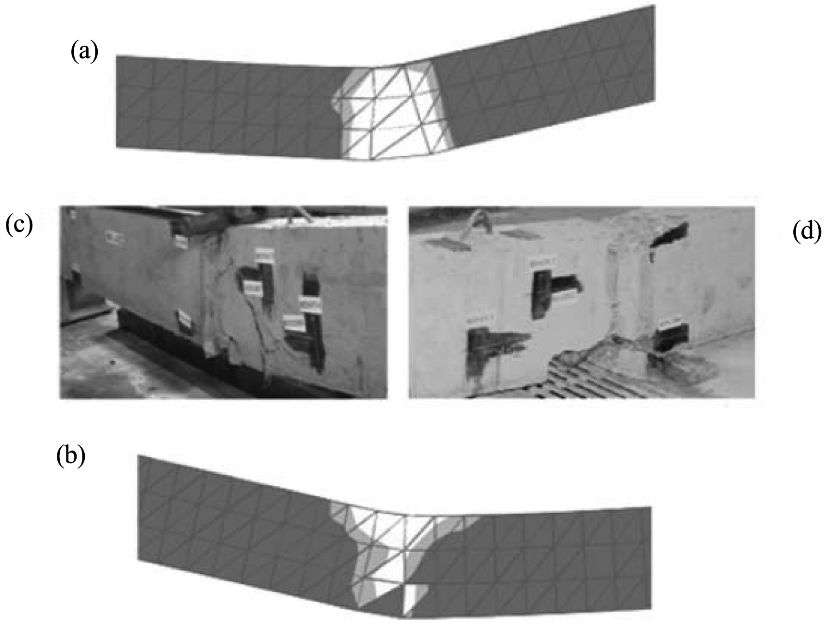

Fig. 10 (a) Tensile damage of concrete in nonlinear analysis (b) compressive damage of concrete in nonlinear analysis (c) failure in test 1 (d) failure in test 2

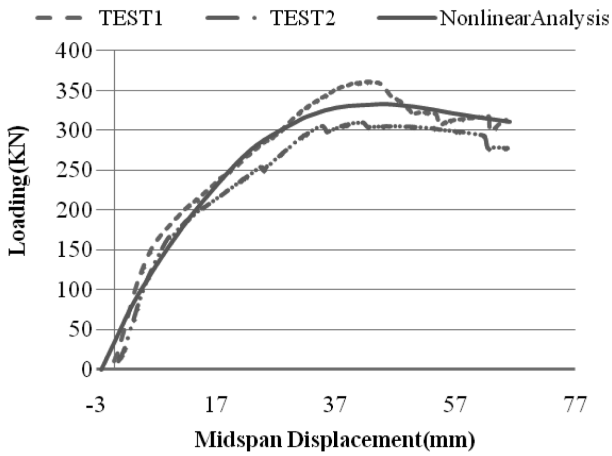

Fig. 11 Load deflection of mid span from numerical and experimental results

6. Nonlinear analysis of models

The hypotheses for the development of continuous stress fields can be implemented in an effective way using the finite element method (FEM) as introduced by Ruiz and Muttoni (2008).

This method is consist of a group of reduction factors to convert concrete compressive strength to equivalent concrete plastic strength or reduction factors for the presence of the duct in concrete beam webs. As discussed by Ruiz and Muttoni (2007) the concrete stress-strain response is

Table 5 Compressive strut angle AUT University tests

	Compressive Strut Angle	
	Test results	Analysis results
Points		
S1,2	43	40
S3,4	37	33
S5,6	21	15
S7,8	26	25

considered elastic perfectly plastic in compression and the tensile strength of concrete is neglected.

But in this paper, nonlinear analysis performed by using concrete damage plasticity theory and as shown in Fig. 13, accurate geometric properties of models include the prestressing tendon duct is considered in the models. In spite of the differences between the finite elements methods described above the compressive strut angles are obtained by means of Mohr's circle as shown in Fig. 9 for both methods.

To evaluate the formation and slope of compressive struts in prestressed concrete beams, various models of PC beams with or without vertical prestressing and having parabolic tendon profile are selected and analyzed using the finite element method. The characteristics are given in Table 6. In this table, the symbol R-C stands for reinforced concrete, P-C for prestressed concrete, P-C with V-P for prestressed concrete with vertical prestressing, P-S stands for prestressed stirrups and C-S for critical sections. A sample of finite element meshes for the models is shown in Fig. 13.

The analysis is performed by considering nonlinear behavior of the materials. Modified 3 dimensional cubic solid elements with 8 nodes (C3D8R) and 3 dimensional truss elements with 2 nodes (T3D2) is used for modeling the concrete and reinforcement respectively. Embedded element technique is used to define interaction between steel and concrete.

The concrete material is defined based on concrete damage plasticity by means of experimental stress-strain diagrams based on Lee and Fenves (1998) researches. In summary, the elasto-plastic response of the concrete damaged plasticity model is described in terms of the effective stress and the hardening variables

$$\overline{\sigma} = D_0^{el}:(\varepsilon - \varepsilon^{pl}) \in \{\overline{\sigma} | F(\overline{\sigma}, \tilde{\varepsilon}^{pl}) \le 0\} \tag{2}$$

$$\dot{\tilde{\varepsilon}}^{pl} = h(\overline{\sigma}, \tilde{\varepsilon}^{pl}) \cdot \dot{\varepsilon}^{pl} \tag{3}$$

Where $\overline{\sigma}$ is the effective stress which is equivalent to the Cauchy stress σ. When damage occurs, however, the effective stress is more representative than the Cauchy stress because it is the effective stress area that is resisting the external loads.

In these relations D_0^{el}, ε and ε^{pl} are initial (undamaged) elastic stiffness of the material, total strain and plastic strain respectively.

Also $\dot{\tilde{\varepsilon}}^{pl}$, $\dot{\tilde{\varepsilon}}^{pl}$ and $\dot{\varepsilon}^{pl}$ are equivalent plastic strain, the plastic part of the strain rate and equivalent plastic strain rate respectively.

F obey the Kuhn-Tucker conditions: $\dot{\lambda}F = 0$; $\dot{\lambda} \ge 0$; $F \le 0$. The Cauchy stress is calculated in terms of the stiffness degradation variable, $d(\overline{\sigma}, \tilde{\varepsilon}^{pl})$, and the effective stress as

$$\sigma = (1-d)\bar{\sigma} \tag{4}$$

Plastic flow is governed by a flow potential G according to the flow rule

$$\dot{\varepsilon}^{pl} = \dot{\lambda}\frac{\partial G(\bar{\sigma})}{\partial \bar{\sigma}} \tag{5}$$

Where $\dot{\lambda}$ is the non-negative plastic multiplier. The plastic potential is defined in the effective stress space.

The constitutive relations for the elasto-plastic response, Eq. (2), are decoupled from the stiffness degradation response, Eq. (4), which makes the model attractive for an effective numerical implementation. The steel material is also defined based on classical metal plasticity using Von Mises yielding surface and stress-strain diagrams as input data.

The effect of prestressing tendon consists of two inclined concentrated forces at the end of beams and a uniformly distributed upward load in the direction of tendon. Vertical prestressing is used as initial condition. In order to increase the accuracy of results, the element dimensions are reduced in the tendon area.

In order to apply vertical prestressing on specimens, this force is exerted on rods by tensile forces owing to tightening of nuts which can be controlled by the externally applied torque. If the friction coefficient is assumed to be constant, the relation between the externally applied torque T and tensile force N acting on a rod can be written as follows (Kim and Yang 2007)

$$T = k.d_b.N \tag{6}$$

Where d_b is rod diameter and k is a torque coefficient dependent on the friction coefficient and geometrical conditions of thread in rods and nuts. The accurate amount of required prestressing rods in each model is evaluated using a finite element method based on above mentioned procedure. The vertical prestressing is considered by means of initial condition (stress type). A schematic view of the prestressed concrete beam models is presented in Fig. 12. The effect of vertical prestressing on load capacity of prestressed concrete beams could be explained by evaluating maximum load capacity ratio.

Geometrically nonlinear static problems sometimes involve buckling or collapse behavior, where the load-displacement response shows a negative stiffness, and the structure must release strain energy to remain in equilibrium. There are several approaches to consider second-order and large displacement effects to predict the nonlinear response of prestressed concrete as applied by Lou and Xiang (2010).

These methods can applied to simulate the post-peak behavior of the member taking into account the strain reversal in non-prestressed steel and concrete at the descending branches of the stress-strain curves as performed by Au *et al.* (2009). Among these analysis methods the modified Riks allows you to find static equilibrium states during the unstable phase of the response. In this study to include nonlinear material and geometry the Riks method is used.

After defining the F.E models and their boundary and loading conditions, different models are analyzed and considering the results, the direction of compression struts and bending strength are determined in order to clarify effects of vertical and horizontal prestressing on the behavior of PC beams. A summary of load capacity and mid span deflection of numerical models has been presented in Table 7.

As shown in Fig. 14, more reduction in shear span to depth ratio, more increase in load capacity

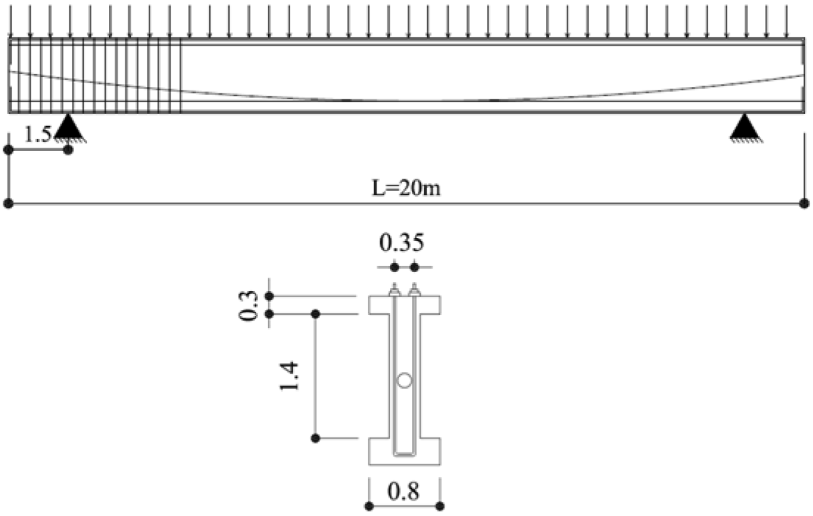

Fig. 12 General view of one of the prestressed concrete beam model

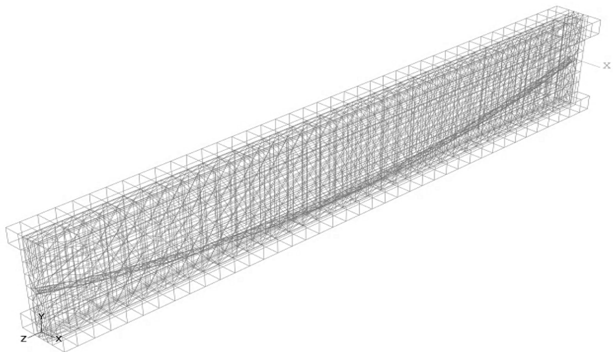

Fig. 13 Finite element mesh of model O-S

Table 6 Geometric properties of numerical models
In this table P-S means prestressed stirrups, c-s means critical sections

Beam type	Beam name	Simple-T	Simple-I	P-S	(a/d)
R-C	R-C-T-S	√			6.66
R-C	R-C-I-S		√		4.11
R-C	R-C-O-S		√		2.21
P-C	T-S	√			6.66
P-C	I-S		√		4.11
P-C	O-S		√		2.21
P-C WITH V-P	POST T-S	√		d = 12 @ 500	6.66
P-C WITH V-P	POST I-S		√	d = 12 @ 2500	4.11
P-C WITH V-P	POST O-S		√	4-d = 12 in c-s	2.21

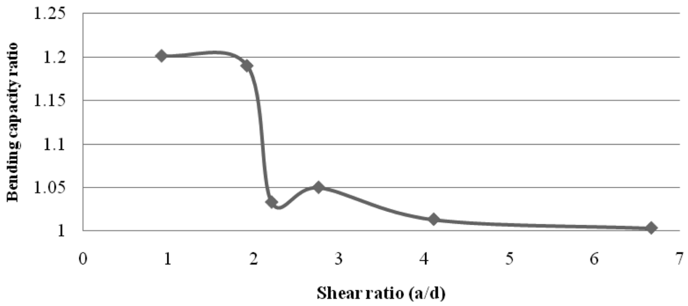

Fig. 14 Bending capacity increase with vertical prestressing in relation to shear ratio

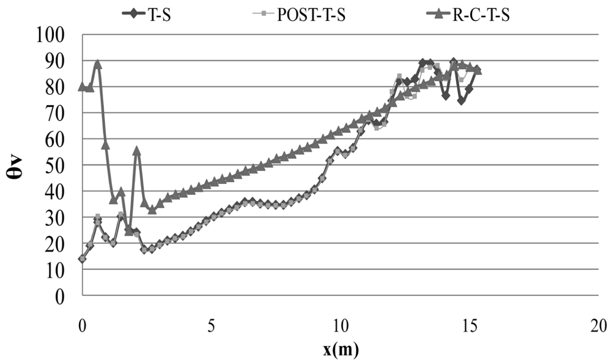

Fig. 15 Compressive strut angle along T-S simple models

Table 7 A summary of numerical results

Name	Failure mode			Maximum and minimum strut angle in shear span (degrees)	Maximum mid span deflection (mm)	Maximum bending capacity (KN/m)
	Tensile shear	Diagonal	Flexural			
R-C-T-S			√	$23 \leq \theta \leq 43$	96	33.03
R-C-I-S		√		$40 \leq \theta \leq 49$	25.43	151.37
R-C-O-S		√		$19 \leq \theta \leq 32$	11	294.384
T-S			√	$19 \leq \theta \leq 40$	96.62	80.377
I-S		√		$20 \leq \theta \leq 34$	25.44	553.879
O-S		√		$10 \leq \theta \leq 19$	11	760.2
POST T-S			√	$19 \leq \theta \leq 40$	386.5	80.64
POST I-S		√		$20 \leq \theta \leq 33$	86.28	561.229
POST O-S		√		$10 \leq \theta \leq 18$	18	760.3

of the beams. In deep beams this increase reaches more than 20%.

The compressive strut angles along the beams axis are determined based on stress field theorem. A summary of maximum and minimum angle value in shear span zone is presented in Table 7.

As shown in Fig. 15, by moving from supports to mid span, compressive strut angle increase. The effect of vertical prestressing on compressive strut angle in deep beams is more than the models with more shear span to depth ratio.

7. Comparison of results with codes' formulas

The shear design methods in concrete beams, using the truss models, consist of the following two stages:

a) Determination of the necessary shear reinforcement

b) Control of the compressive stress in diagonal compression struts.

The compression strut slopes derived from nonlinear analysis, the code relations, and experimental results are studied and compared.

7.1 Orientation of compression struts

A significant study was performed on 43 prestressed beams with *I* and *T* sections by Elzanety *et al.* (1988). In these experiments the gradual change of the crack angles from 20° to 35° was observed. Also in research performed by Kaufman and Ramirez (1988), the value of this angle is reported from 15° to 35°. According to Mahtomedi (1998), the experiments conducted by various researchers declare a gradual, increase in crack slopes from the support zone toward the mid-span, varying from 17° to 40°.

Using the code relations shown in Table 8, the compressive strut slope is investigated and compared with nonlinear analysis results on uniformly loaded beams. The variables used in Table 8 are defined as follows:

A_c = cross sectional area of tendon,
b_n = effective width of web,
f_{cd} = concrete design strength,
P_e = effective prestressing force,
V_P = shear force carried by prestressing tendon,
V_D = live load shear force,
V_L = dead load shear force,
$V_{u,\max}$ = maximum shear strength of the beam,
$V_{u,\min}$ = minimum shear strength of the beam,
V^* = existing shear force,
$\sigma_{cp,\mathrm{eff}}$ = average effective stress in concrete due to axial load,
Φ = strength reduction factor,
z = coordinate; lever arm of internal forces.

According to the nonlinear analysis results the lower limit of compressive strut angle in prestressed concrete beams is about 15 degrees. In ACI (2005) Compressive strut slope is 45 degrees which is very conservative. The Grasser method which is based on B.S (2004) is most affected by horizontal prestressing force. Since $\sigma_{cp,\mathrm{eff}}$ values are changed by tendon slope variations so the compressive strut angle will be variable along the beam length. In the French code and AS (1988) vertical prestressing and vertical component of prestressing in parabolic tendons are considered by using V_P in compressive strut slope relations, which is similar to straight stress field method.

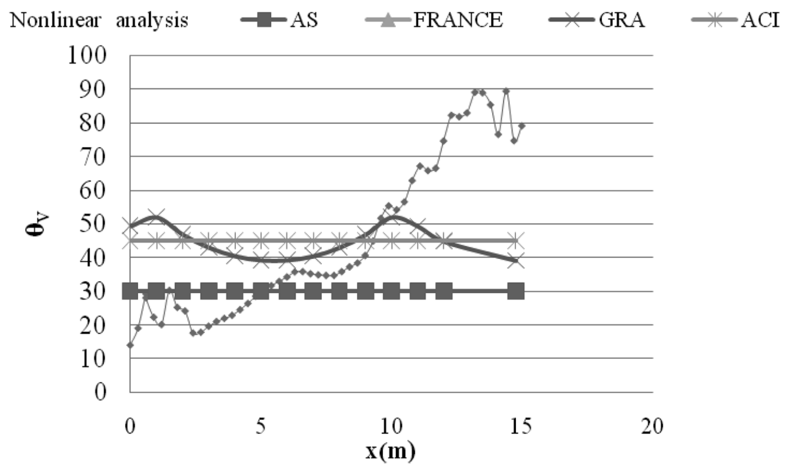

Fig. 16 Compressive strut angle in codes and papers in comparison with nonlinear analysis in POST-T-S model

Fig. 16 compares compressive strut slope in codes and nonlinear analysis. This slope can be calculated using continuous stress field, which is based on Mohr's circle and as shown in Fig. 15 experimental results confirm it's precision.

8. Recommendation for compression strut inclination

Considering the nonlinear analysis results on flanged section (*I* or *T*) beams under uniform loading, with minimum web reinforcement ratio and with parabolic ducts and comparing them with experimental studies, the s-shape graph as shown in Fig. 17 is proposed for determination of θ angle along the shear span of simple beams.

If θ_i and θ_f are the angles of the strut slope at the beam supports (x = 0) and mid span (x = 0.5L),

Table 8 A summary of relations

Codes and methods	Compressive strut angle (θ)	Allowable limits of (θ)
ACI, EC2A	45°	45°
EC2B(GRASSER)	$\theta = \cot^{-1}\left(1.25 + 3\dfrac{\sigma_{cp,\text{eff}}}{f_{cd}}\right)$	$22° \le \theta \le 68°$
AS-3600-1988	$\theta = 30 + \dfrac{15(V^* - \phi V_{u,\min})}{\phi V_{u,\max} - \phi V_{u,\min}}$	$30° \le \theta \le 45°$
French Code	$0.5\tan^{-1}\left[\dfrac{1.25V_D + 1.5V_L - V_P}{b_n \cdot z \cdot \dfrac{p_e}{A_C}}\right]$	$30° \le \theta \le 45°$

respectively the value of θ at any section with distance x from the support can be determined as below

$$\theta = \begin{cases} \theta_i + \left(\frac{\theta_f - \theta_i}{2}\right)\left(\frac{x}{0.2L}\right)^4 & 0 \le x \le 0.2L \\ \theta_i + \left(\frac{\theta_f - \theta_i}{2}\right)\left(\frac{5}{2} - \frac{10x}{3L}\right)^5 & 0.2L \le x \le 0.5L \end{cases} \tag{12}$$

The value of θ_i and θ_f are computed from Table 9 and Table 10 and depend on the loading point at the section. The variable used in Table 9 and 10 are defined as follows

V = shear force at the support point,
V_P = vertical component of the tension in inclined prestressing tendon,
b_w = effective web width, taken as the flexural level arm, but which need not to be taken less than 0.9 d,
M = moment at mid span,
N = axial load at mid span, taken as positive if tensile and negative if compressive,
A_P = area of prestressed longitudinal reinforcement on tension side of the member,

Table 9 Value of θ_i

$\frac{V - V_P}{(b_w \cdot Z \cdot f_c')}$	0.03	0.045	0.06	0.075	0.09	0.12	0.15
θ_i	27	27	23.5	23.5	25	27.5	30

Table 10 Value of θ_f

$\frac{(M/Z + 0.5N - 1.1A_P f_P)}{E_S A_S + E_P A_P}$	0	0.001	0.0015	0.002
θ_f	36	36	41	43

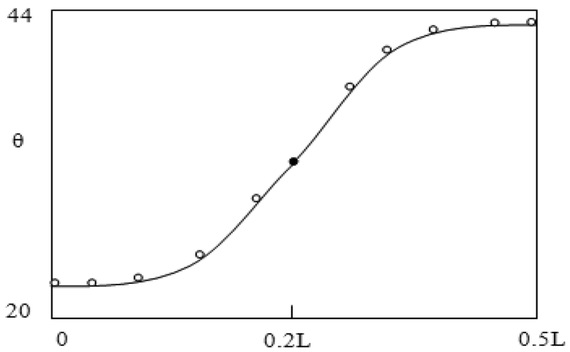

Fig. 17 The two-part curve of compression strut slope

A_s = area of non-prestressed longitudinal reinforcement on the tension side of the member,
f_p = effective stress in the prestressing tendon,
E_s = modulus of elasticity of reinforcing bars,
E_p = modulus of elasticity of prestressing tendons.

To evaluate the range of the presented equation, the analytical results of different models have been compared with suggested relation and codes' formulas which has a 5 percent difference. So this relation can be used with a good accuracy in determination of strut's slope in simple prestressed beams with above mentioned characteristics.

9. Conclusions

This paper presents the results of theoretical and experimental research on the behavior of post-tensioned beams with vertical prestressing. Two full-scale tests performed on girders failing in shear are presented. Their experimental results are used to verify numerical modeling.The main findings of the numerical study are:

1- The ability of a given stress field to reproduce the actual behavior (and strength) of member is significantly influenced by its strain compatibility. The most compatible stress fields are those that present a smooth variation of the stresses between adjacent struts, so-called continuous stress fields.

2- Muttoni, Fernandez and AUT laboratory test results confirm the validation of nonlinear analysis especially in load capacity, maximum mid span deflection and compressive strut angle estimation.

3- By moving from supports to mid span, compressive strut angle increase. Generally compressive strut slope is higher in the PC beams with more shear span to depth ratio.

4- Horizontal prestressing has an impressive effect on compressive strut angle variation along the beam and reduce it to 60% in some cases. This reduction depends on effective prestressing force. Vertical prestressing influences are considerable just in load capacity and shear strength of beams with lower shear span to depth ratio and deep beams particularly. Vertical prestressing in beams with critical shear behavior (i.e. deep beams), cause up to 20% increase in load capacity, and reduce compressive strut angle.

References

American Concrete Institute (ACI) (2005), *Building Code Requirements for Structural Concrete (ACI_318_05)*, Farmington Hills.

Au, F.T., Chan, K.H., Kwan, A.K. and Du, J.S. (2009), "Flexural ductility of prestressed concrete beams with unbonded tendons", *Comput. Concrete,* **6**(6), 451-472.

Bentz, C.E., Vechio, J.F. and Collins, M.P. (2006), "Simplified modified compression field theory for calculating shear strength of reinforced concrete elements", *ACI Struct. J.,* **103**(4), 614-624.

British Standards Institution (2004), *The European Standard EN 1992-1-1, Eurocode2: Design of Concrete Structures (EC2)*, Brussels, Belgium.

Brown, M.D. and Oguzhan, B. (2006), "Minimum transverse reinforcement for bottle-shaped struts", *ACI Struct. J.,* **103**(6), 813-821.

Collins, M.P. and Mitchell, D. (1980), "Shear and torsion design of prestressed and nonprestressed concrete

beams”, *J. PC. Inst.*, **25**(5), 32-100.
Comite Euro-International du beton (CEB) (1990), *CEB-FIP Model Code 1990*, Bulletin D' Information N0.195, Paris.
Czaderski, C. and Motavalli, M. (2006), “Determining the remaining tendon force of a large-scale, 38-Year-Old prestressed concrete bridge girder”, *PCI J.,* **51**(4), 56-68.
Elzanety, A.H., Nilson, A.H. and Slate, F.O. (1988), “Shear capacity of prestressed concrete beams using high strength concrete”, *ACI J.,* 359-368.
Kaufman, M.K. and Ramirez, J.A. (1988), “Re-evaluation of the ultimate shear behavior of high-strength concrete prestressed I-beams”, *ACI J.,* 295-303.
Kim, S.Y. and Yang, K.H. (2007), “Tests of reinforced concrete beams strengthened with wire rope units”, *Eng. Struct.*, **29**, 2711-2722.
Lee, J. and Fenves, G.L. (1998), “Plastic-damage model for cyclic loading of concrete structures”, *J. Eng. Mech.,* **124**(5), 892-900.
Lou, T. and Xiang, Y. (2010), “Numerical analysis of second-order effects of externally prestressed concrete beams”, *Struct. Eng. Mech.*, **35**(5), 631-643.
Mahtomedi, M. (1998), “Nonlinear analysis of prestressed concretes in order to evaluate shear strength of sections and result comparison with valid codes”, M.SC Thesis, Amir Kabir University of Technology, Tehran, Iran.
Morsch, E. (1920), *Reinforced Concrete Construction—Theory and Application*, Wittwer, Stuttgart, V. 1, Part 1.
Morsch, E. (1922), *Reinforced Concrete Construction—Theory and Application*, Wittwer, Stuttgart, V. 1, Part 2.
Muttoni, A., Schwartz, J. and Thürlimann, B. (1997), *Design of Concrete Structures with Stress Fields*, Birkhaüser, Boston.
Rabczuk, T., Akkermann, J. and Eibl, J. (2005), “A numerical model for reinforced concrete structures”, *Int. J. Solids Struct.,* **42**, 1327-1354.
Ramirez, J.A. and Breen, G.E. (1991), “Evaluation of a modified truss model approach for beams in shear”, *ACI Struct. J.,* **88**(5), 562-571.
Ritter, W. (1899), “Die bauweise hennebique”, *Schweizerische Bauzei-tung*, **33**(7), 59-61.
Ruiz, M.F. and Muttoni, A. (2007), “On development of suitable stress fields”, *ACI Struct. J.,* **104**(9), 495-502.
Ruiz, M.F. and Muttoni, A. (2008), “Shear strength of thin-webbed post-tensioned beams”, *ACI Struct. J.,* **105**(3), 308-317.
Standards Association of Australia (1988), *Australia Standard for Concrete Structures (AS-3600-1988)*, Sydney.
Talbot, A.N. (1909), *Tests of Reinforced Concrete Beams: Resistance to Web Stresses Series of 1907 and 1908*, Bulletin 29, University of Illinois Engineering Experiment Station, Urbana, Ill, Illinois.
Vechio, F.J. and Collins, M.P. (1986), “The modified compression-field theory for reinforced concrete elements subjected o shear”, *ACI J.,* 219-231.
Wagner, H. (1929), *Metal Beams with Very Thin Webs*, Berlin.
Wang, G.L. and Meng, S.P. (2008), “Modified strut-and-tie model for prestressed concrete deep beams”, *Eng. Struct.,* **30**(12), 3489-3496.
Withey, M.O. (1907), *Tests of Plain and Reinforced Concrete Series of 1906,* Bull. of the University of Wisconsin Eng. Series, Wisconsin.